



Overview: The SPIRE Instrument

Bernhard Schulz
NHSC/IPAC



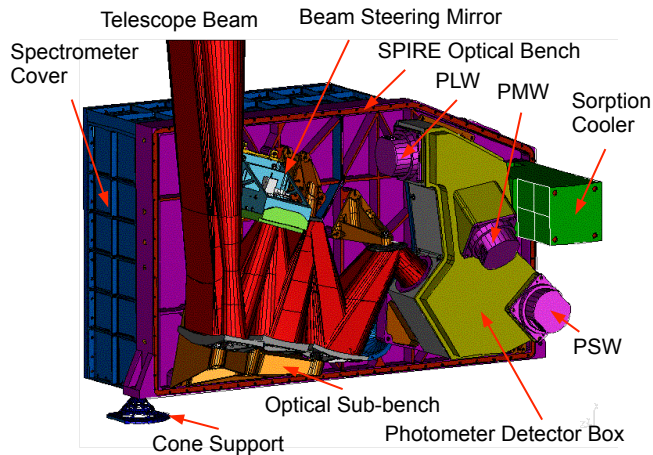


Contents

- SPIRE Introduction
- SPIRE Science examples
- SPIRE Instrument basics
 - Footprint, focal plane geometry, wavelength coverage
- Photometer observing modes ([AOTs](#))
- Spectrometer observing modes ([AOTs](#))
- Calibration
 - Bolometer stability, flux calibration, planetary calibrators, linearisation, accuracies
- Standard processing pipelines
 - Block diagrams, product levels
- Online Demo
 - Retrieve an observation context from pool
 - Look at Level 2 products

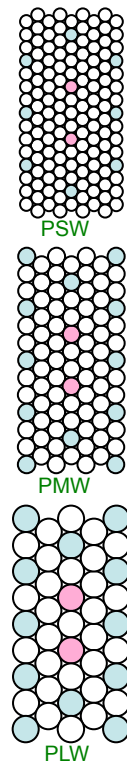
The SPIRE Instrument

Photometer Side



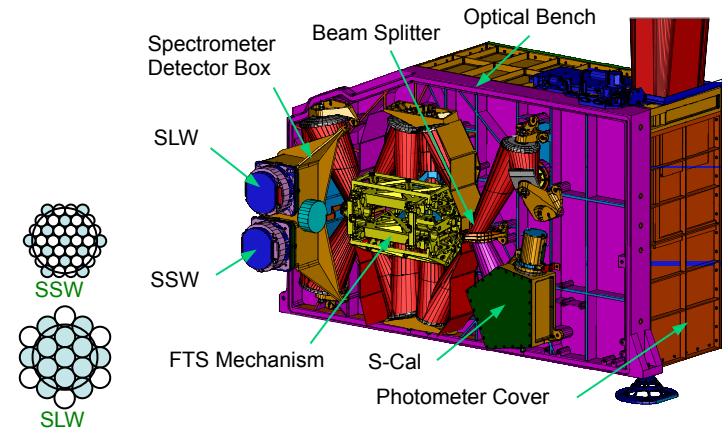
Imaging Photometer

Simultaneous observation in 3 bands
139, 88, and 43 pixels
Wavelengths: 250, 350, 500 μm
 $\lambda/\Delta\lambda \sim 3$
FOV 4' x 8', beams 17.6", 23.9", 35.1"



Highly stable Spider-web bolometer arrays

Spectrometer Side



Imaging Fourier Transform Spectrometer

Simultaneous imaging observation of the whole spectral band
37 and 19 pixels
Wavelength Range: 194-313, 303-671 μm
Resolution: 24.98, 7.207, 1.193 GHz
Circular FOV 2.0' diameter, beams: 17-21", 29-42"

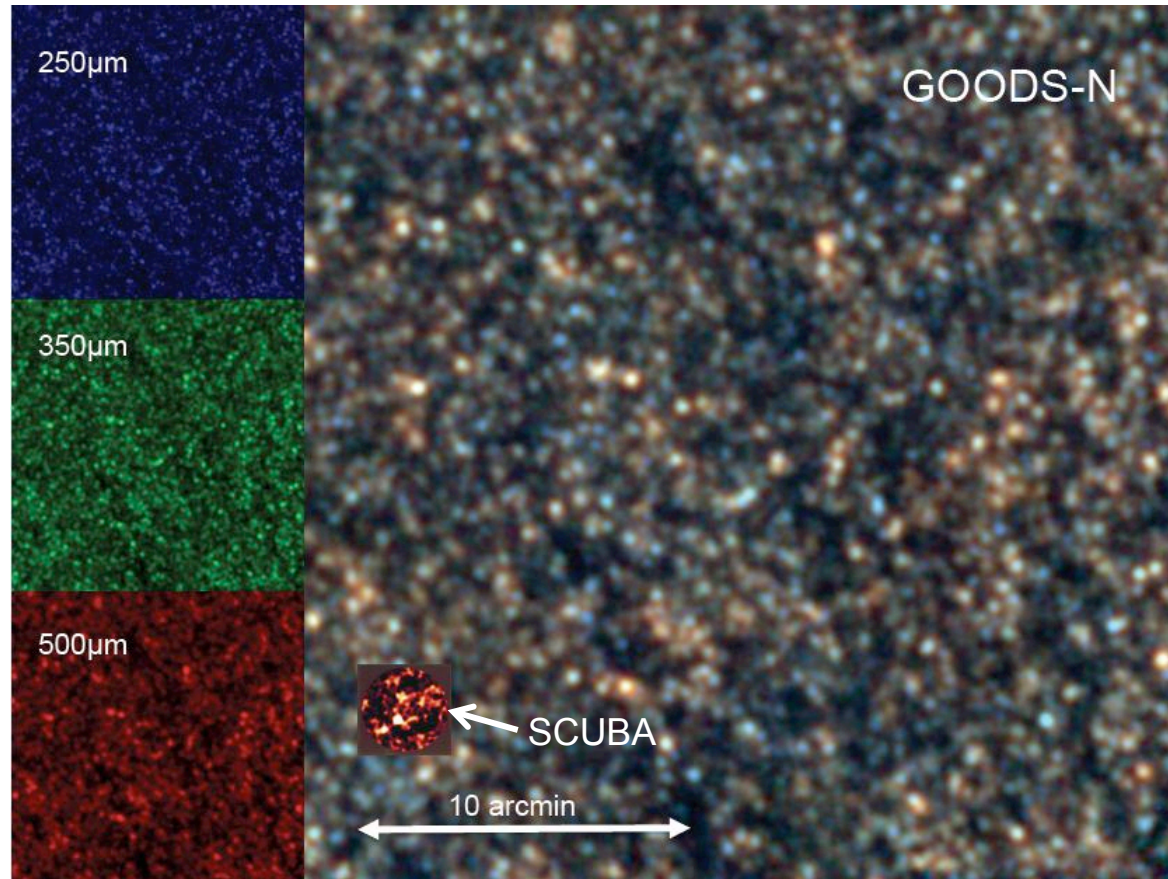


SPIRE Science



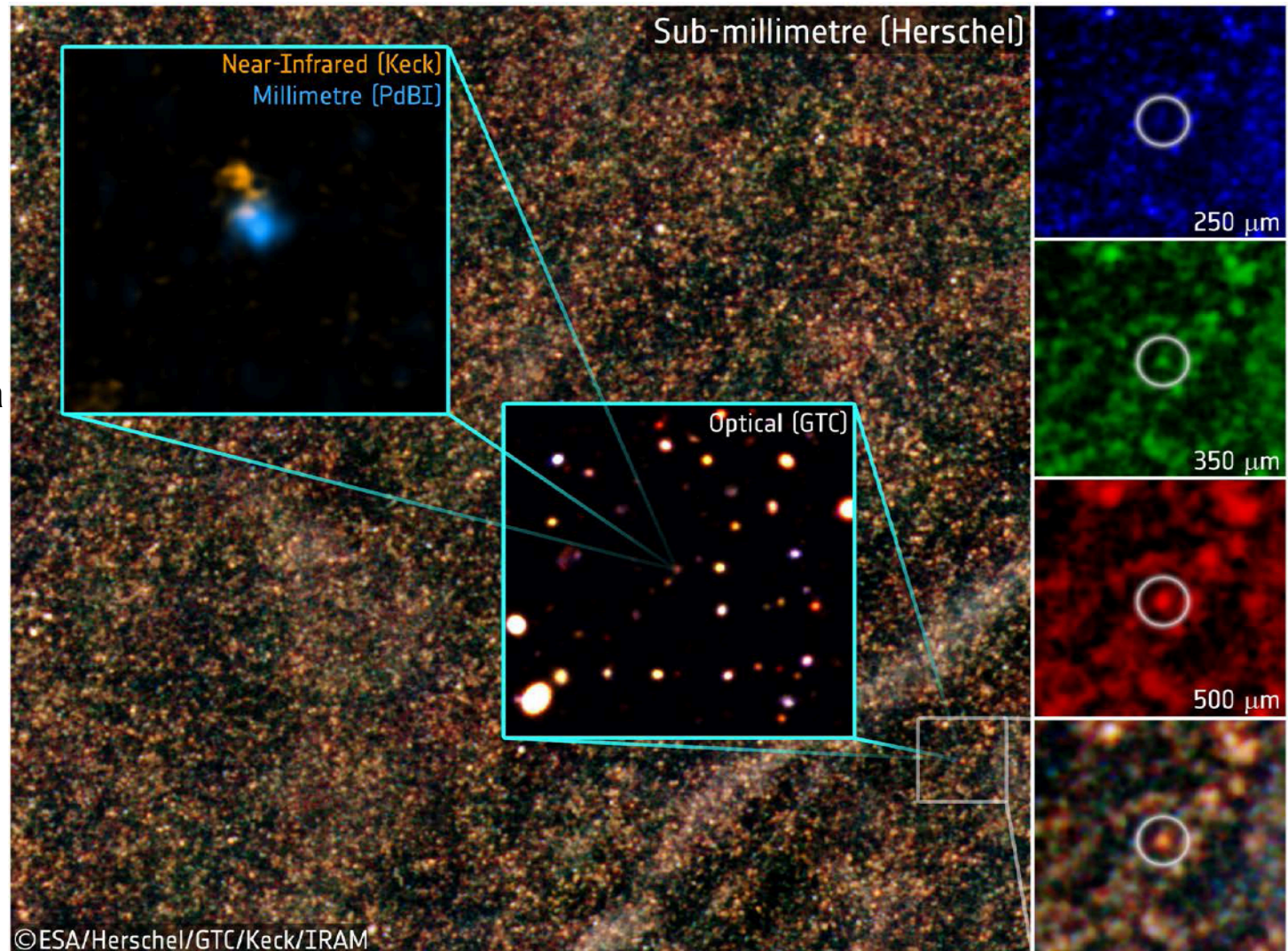
GOODS-North as seen by SPIRE

HERMES





Riechers, D.A. et al., 2013.
A dust-obscured massive maximum-starburst galaxy at a redshift of **6.34**.
Nature, 496(7), pp. 329–333.



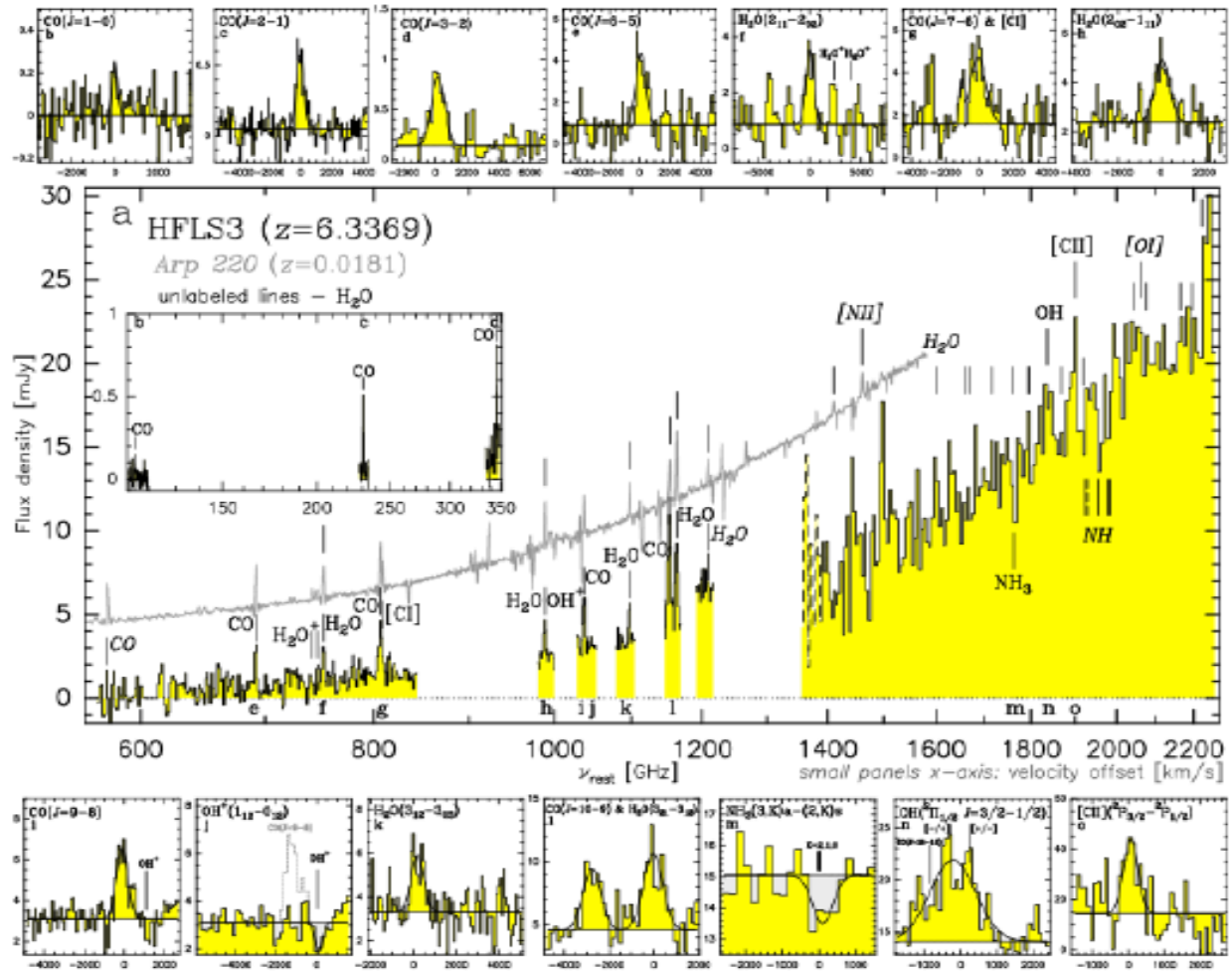


Riechers, D.A. et al., 2013.
A dust-obscured massive
maximum-starburst galaxy
at a redshift of 6.34.
Nature, 496(7), pp.329–
333.

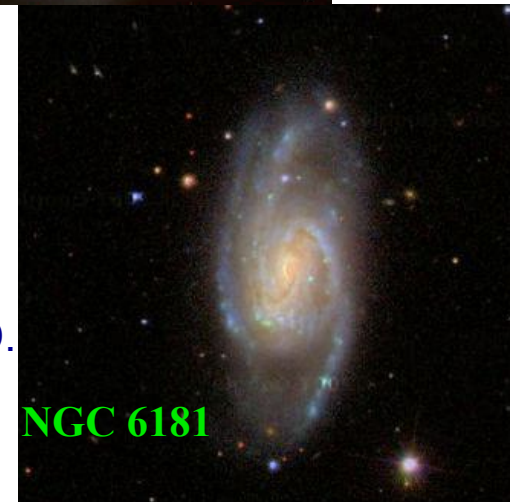
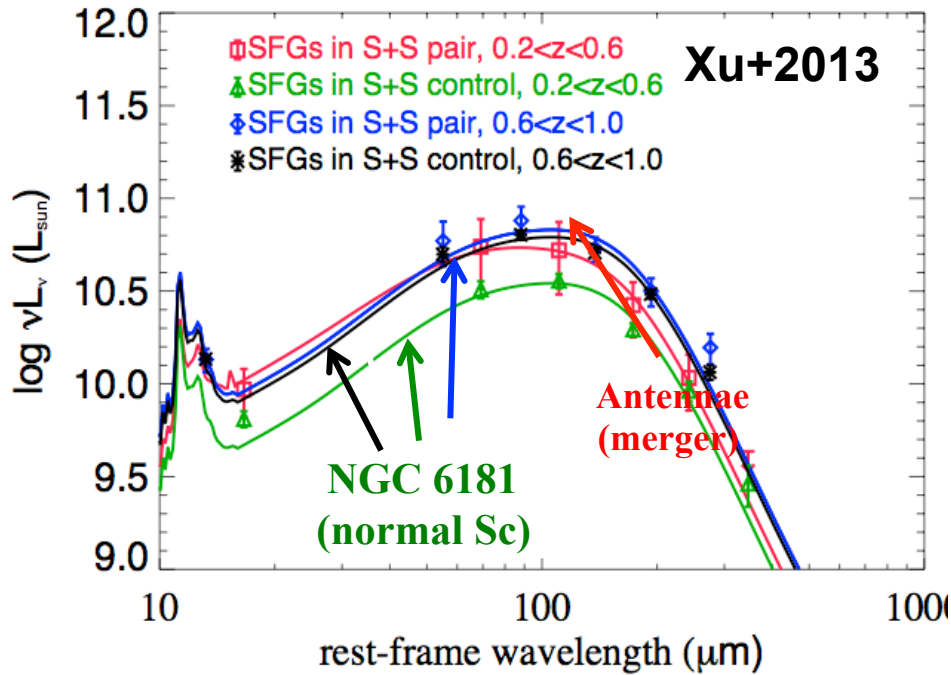
**Comparison of HFLS3 with Arp220
and the Milky Way:**

- Much larger dust and gas masses at comparable stellar masses.
- In HFLS3 40% of the baryonic mass is in the ISM.
- SFR > 2000 times that of the Milky Way already at only 880 Mil years after Big Bang.

	HFLS3	Arp 220*	Milky Way*
redshift	6.3369	0.0181	-
$M_{\text{gas}} (M_{\text{sun}})^a$	$(1.04^{+0.09}_{-0.09}) \times 10^{11}$	5.2×10^9	2.5×10^9
$M_{\text{dust}} (M_{\text{sun}})^b$	$1.31^{+0.32}_{-0.30} \times 10^9$	$\sim 1 \times 10^8$	$\sim 6 \times 10^7$
$M_{\star} (M_{\text{sun}})^c$	$\sim 3.7 \times 10^{10}$	$\sim 3.5 \times 10^{10}$	$\sim 6.4 \times 10^{10}$
$M_{\text{dyn}} (M_{\text{sun}})^d$	2.7×10^{11}	3.45×10^{10}	2×10^{11} (<20 kpc)
f_{gas}^e	40%	15%	1.2%
$L_{\text{FIR}} (L_{\text{sun}})^f$	$2.86^{+0.32}_{-0.31} \times 10^{13}$	1.8×10^{12}	1.1×10^{10}
SFR ($M_{\text{sun}} \text{yr}^{-1}$) ^g	2,900	~180	1.3
$T_{\text{dust}} (K)^h$	$55.9^{+9.3}_{-12.0}$	66	~19



Mean IR SEDs (stacking) of interacting & normal galaxies at different redshifts



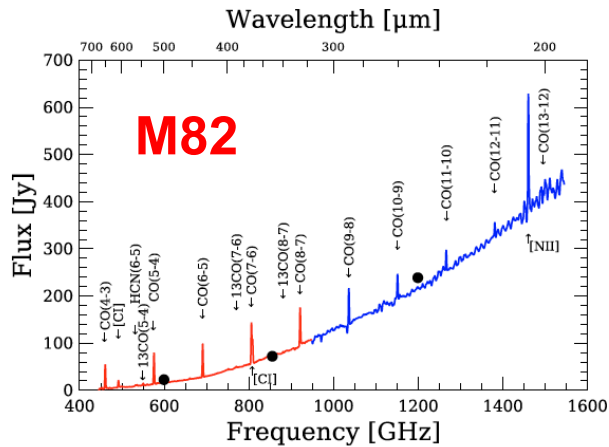
- Interacting galaxies at $z=0.4 \pm 0.2$ (red): can be fit by merger SED.
- Interacting galaxies at $z=0.8 \pm 0.2$ (blue): can be fit by normal SED. (same as that of normal galaxies in the control sample).

Interaction induced SFR enhancement decreases against z !

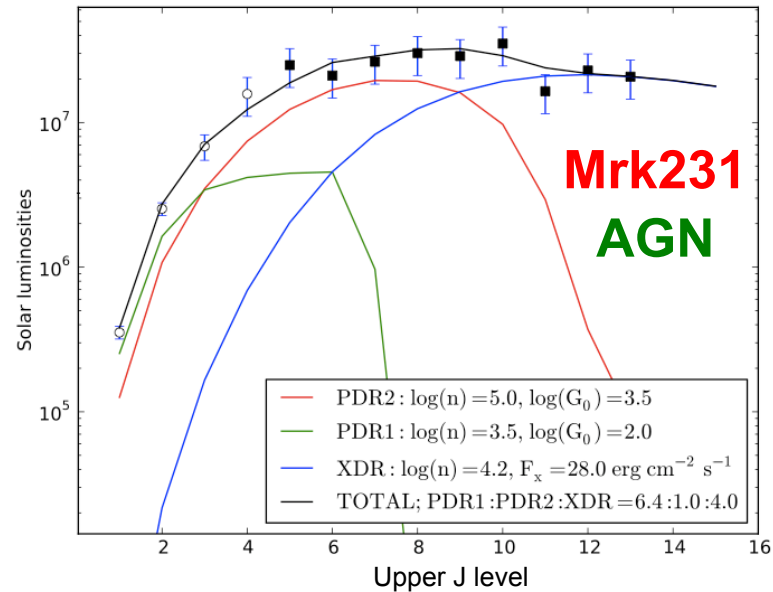
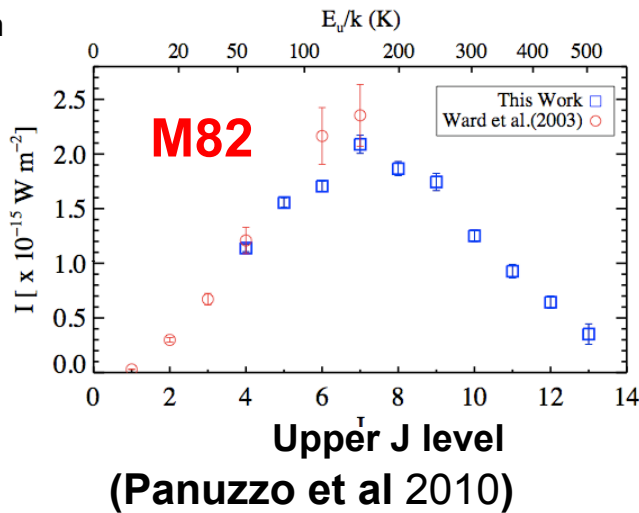


Why CO Spectral Line Energy Distribution (SLED)? Starburst vs. AGN Gas Heating

SB



- CO emission line ladder.
- Radiative transfer modeling.
- Warm gas ~500K in addition to known cold component.



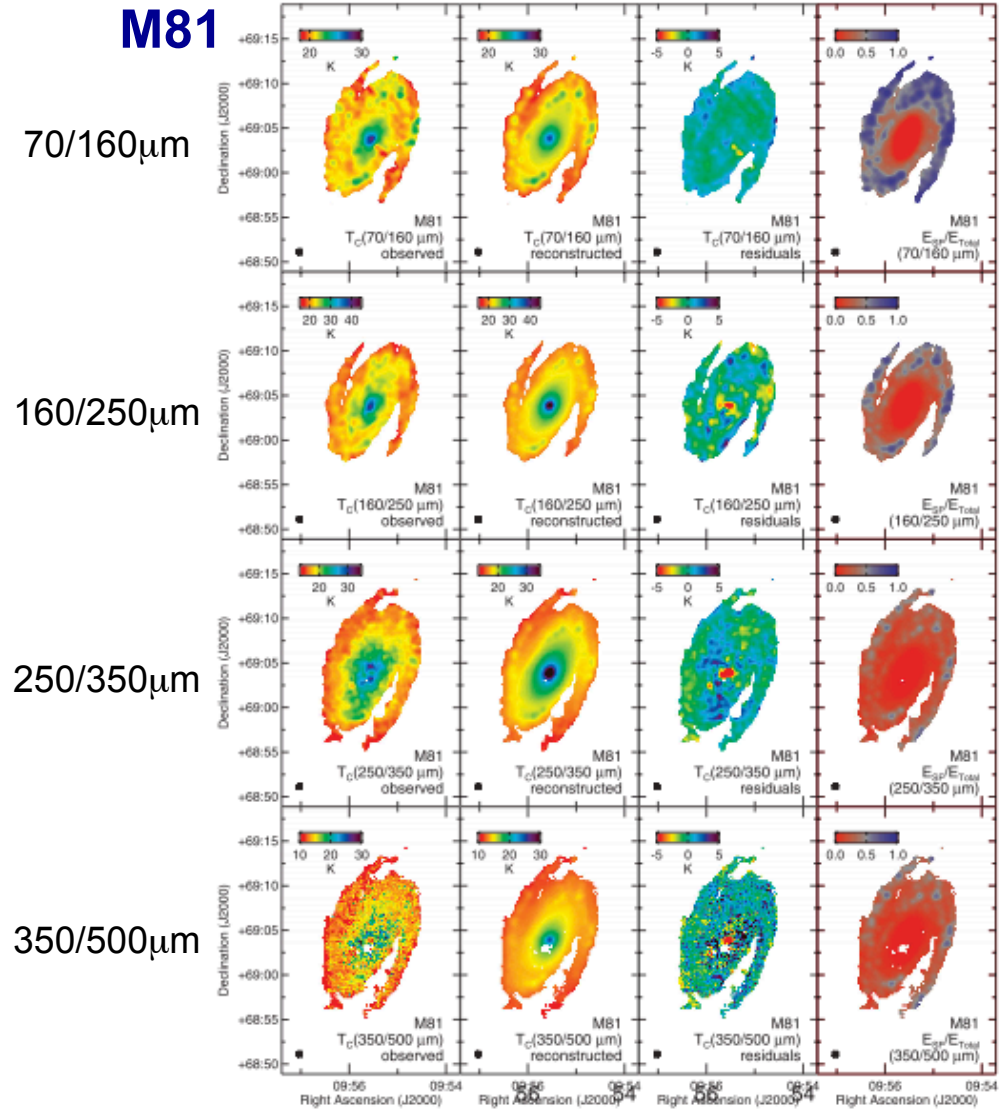
- Detected: CO ladder, H₂O, OH⁺, H₂O⁺, CH⁺, HF
- X-ray driving excitation and chemistry out to 160pc.
- X-rays probably from central AGN.

Striking difference between CO SLED of SB and AGN!

(Van der Werf et al 2010)

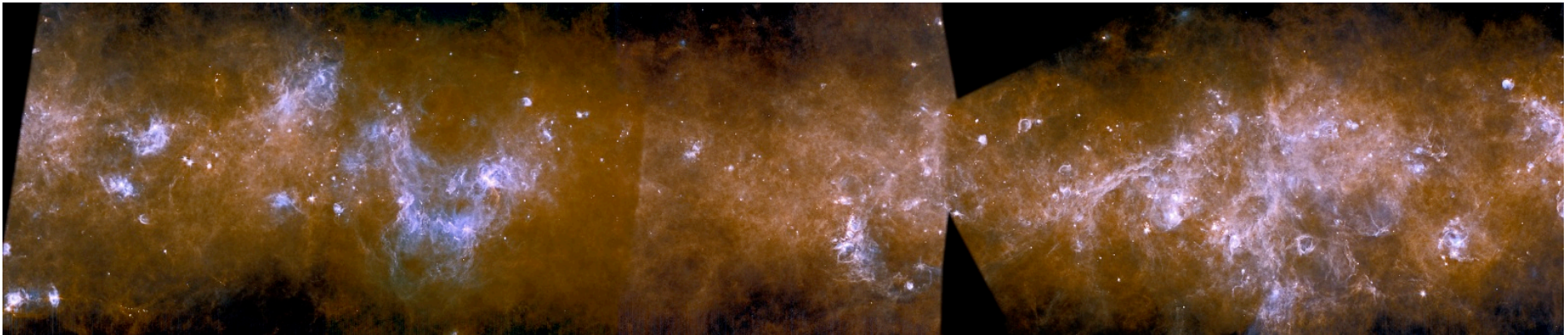
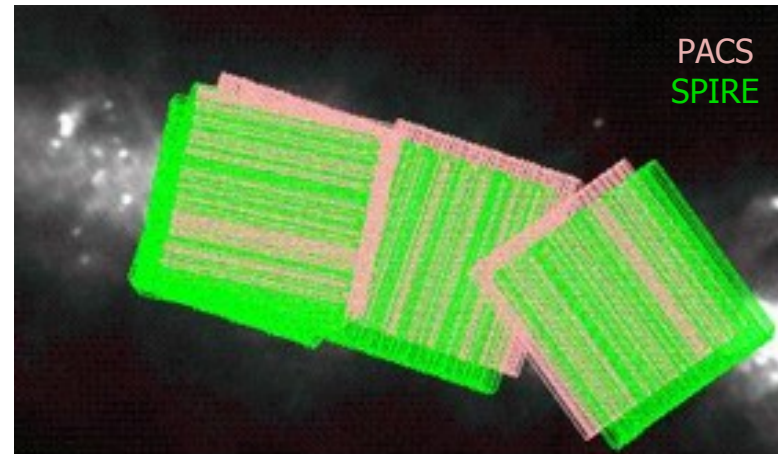


- Investigation of dust heating in M81, M83 and NGC 2403
- Using MIPS 70 μ m, PACS 70-160 μ m, SPIRE 250-500 μ m data, 1.6 μ m 2MASS and H α CCD images.
- 70/160 μ m ratios strongly influenced by SFRs.
- Emission > 250 μ m from cold component that is rather unaffected by SF but more by the total stellar population.
- Impact on radiative modeling.
- Bendo et al. 2012, MNRAS 419, 1833

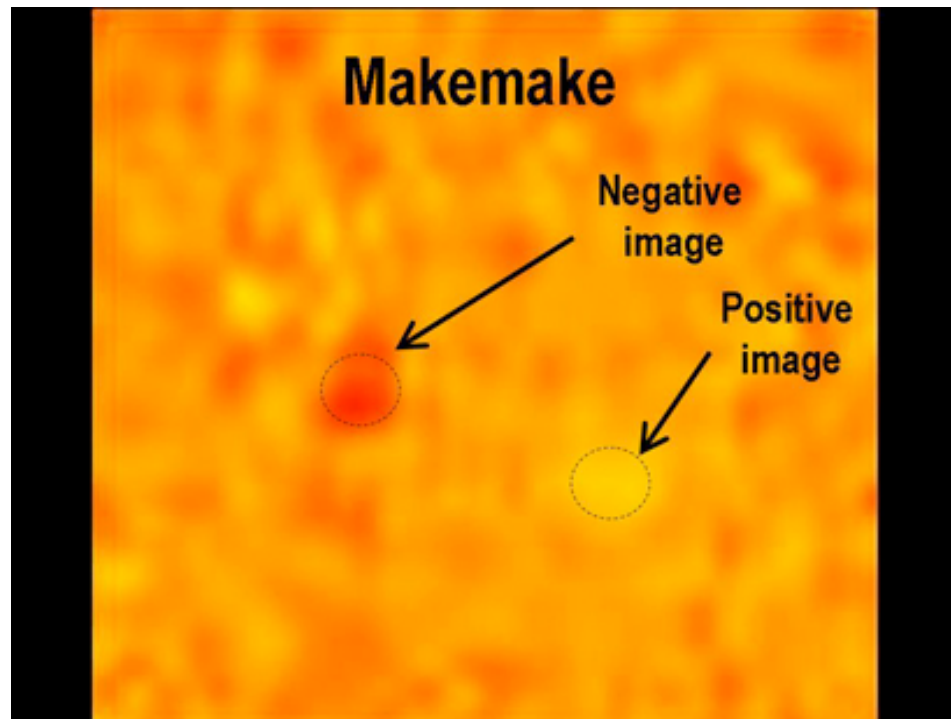


HiGal Survey

- $|b| < 1$ deg covered by square tiles, scanned in two directions.
- Covering entire Galactic plane.



Dwarf Planet 136472 Makemake



Lim et al. 2010, A&A 518, L148

Difference of two observations of dwarf planet Makemake that were made 44 h apart on 01-Dec-2009.

Thanks to the proper motion of the object it appeared as a pair of negative and positive images with fluxes:
 $F(250\mu\text{m}) = 9.5\pm 3.1\text{mJy}$
 $F(350\mu\text{m}) = 7.1\pm 1.8\text{mJy}$

This technique beats very efficiently **confusion noise** (~6mJy).



Many more topics:

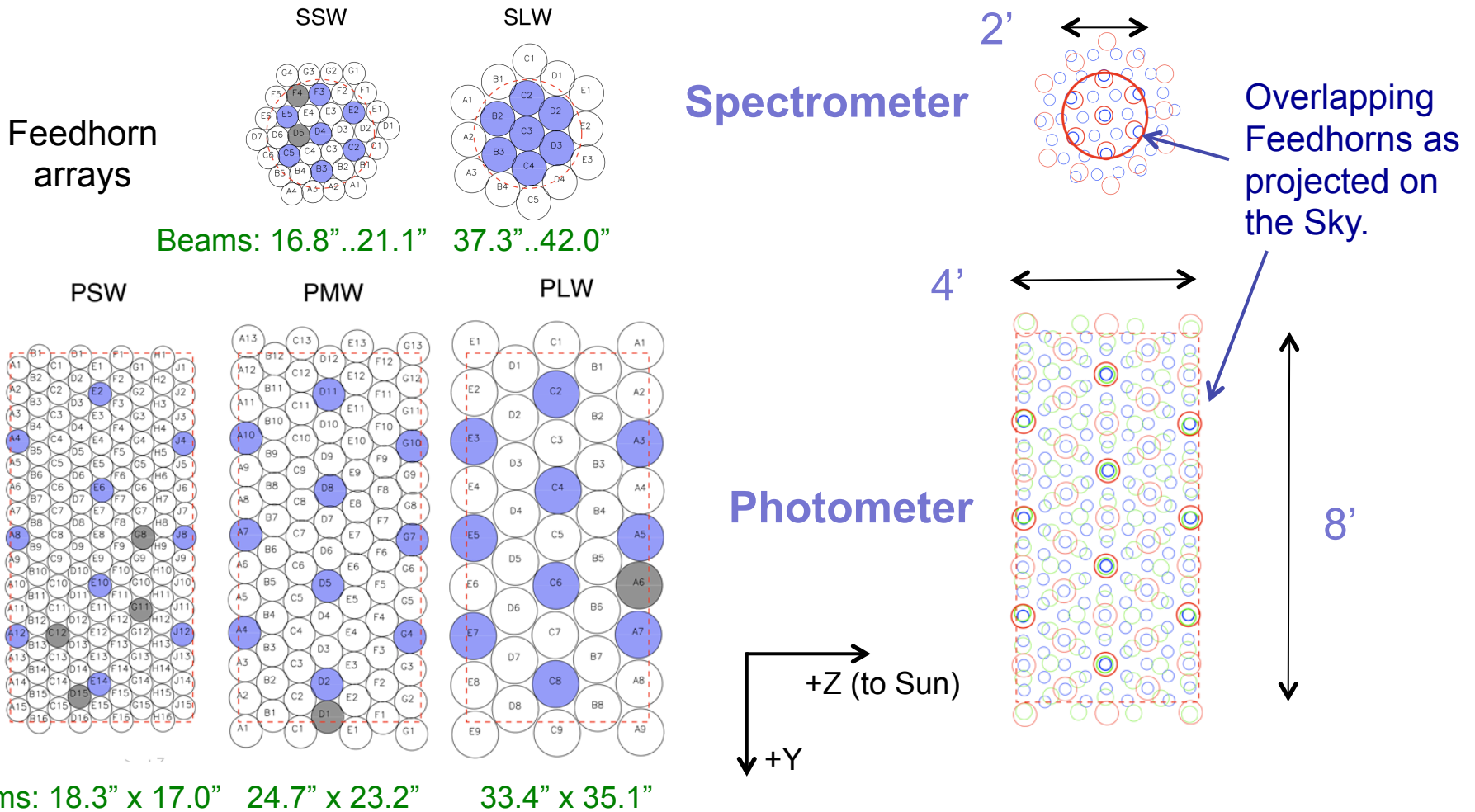
- Lensed galaxies
- M31
- Water and CO in Arp 220
- Spectroscopy of evolved stars
- etc....



Instrument Details

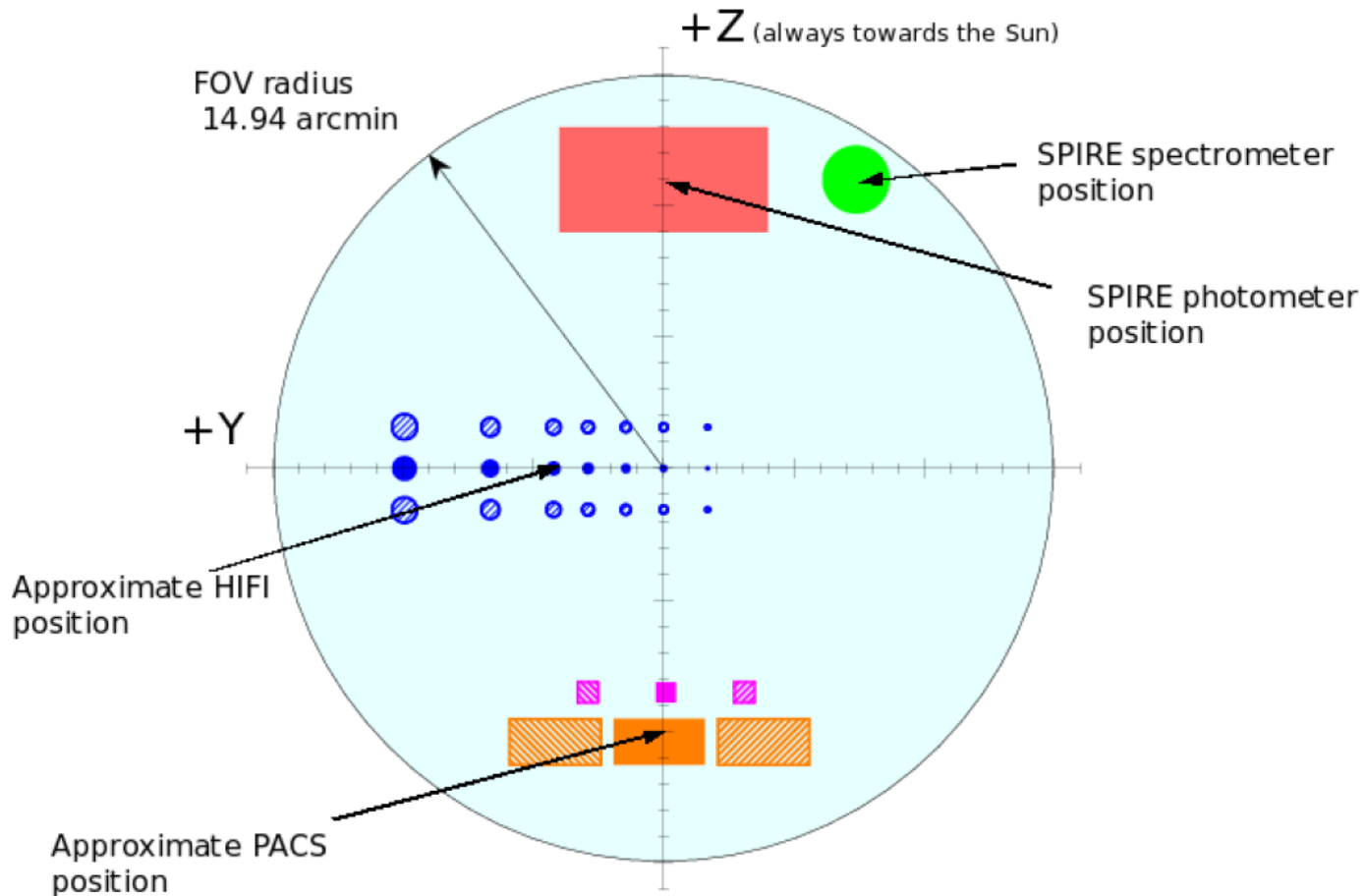


Bolometer Arrays Projected on the Sky



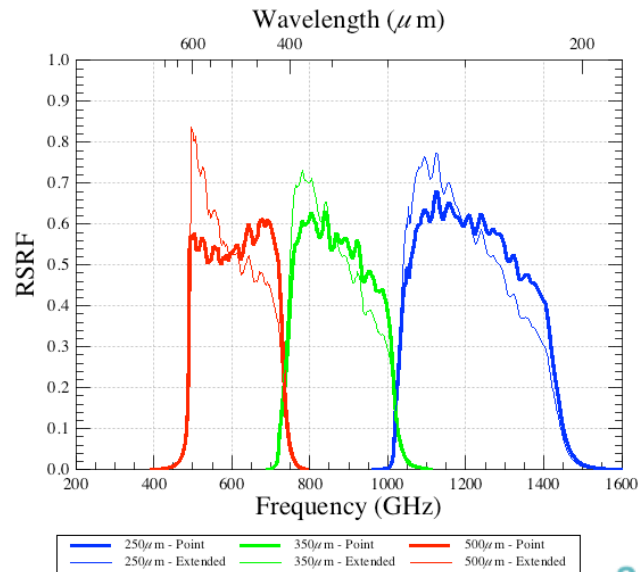


SPIRE in the Herschel Focal Plane



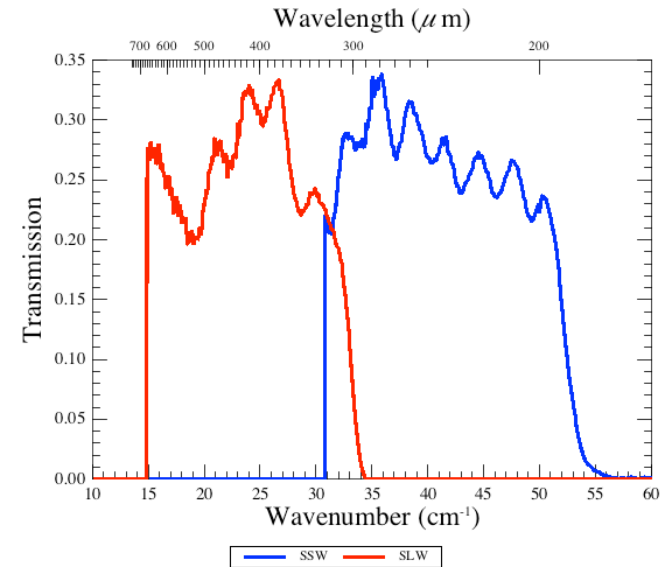


SPIRE Wavelength Coverage

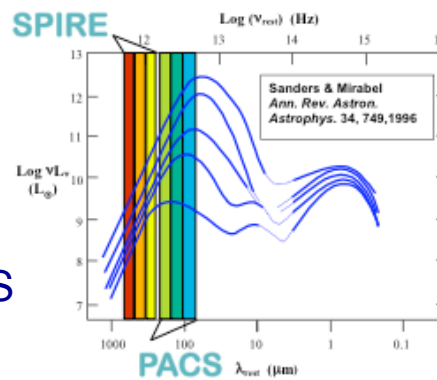


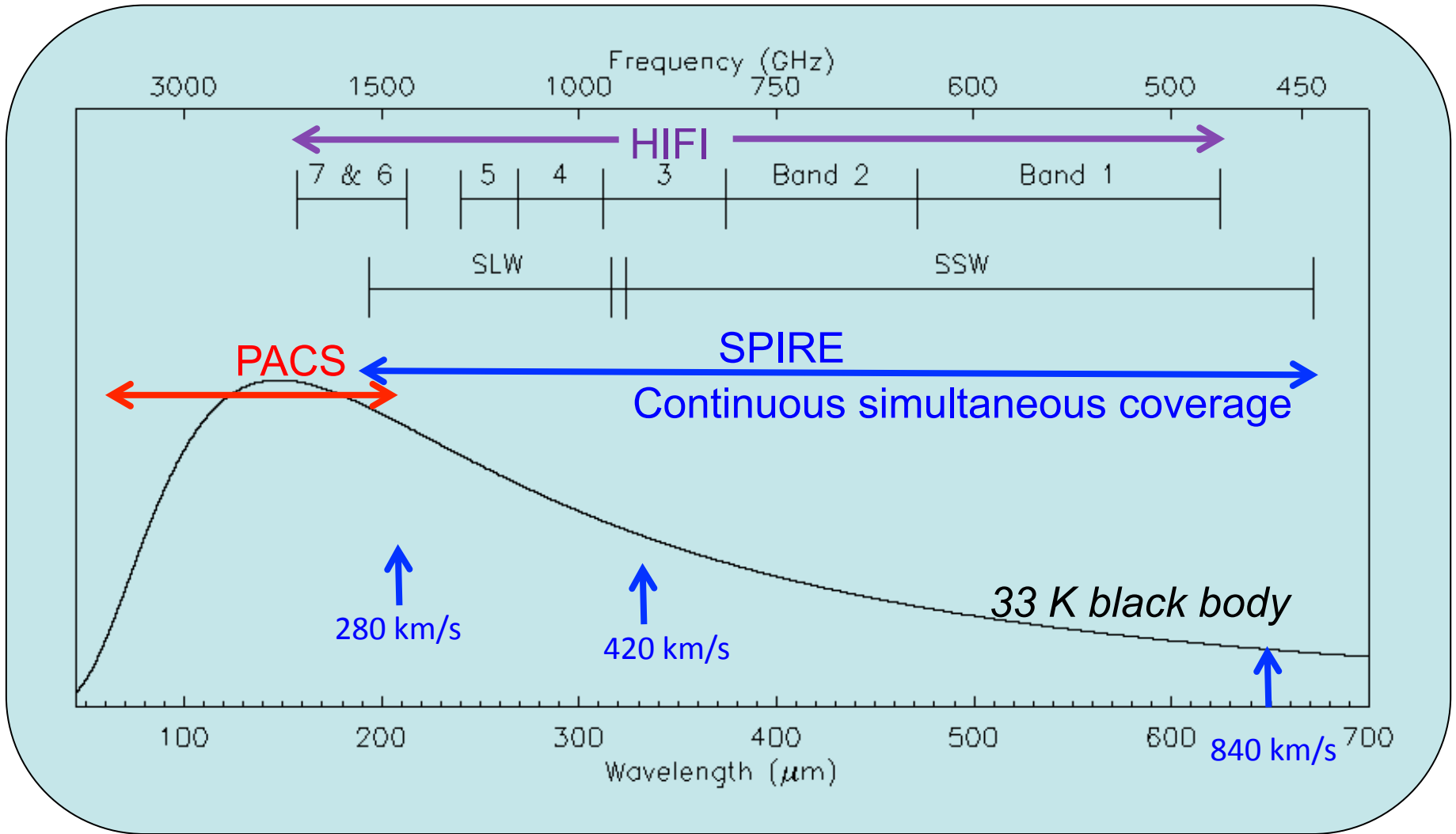
Photometer

Complementary to PACS



Spectrometer







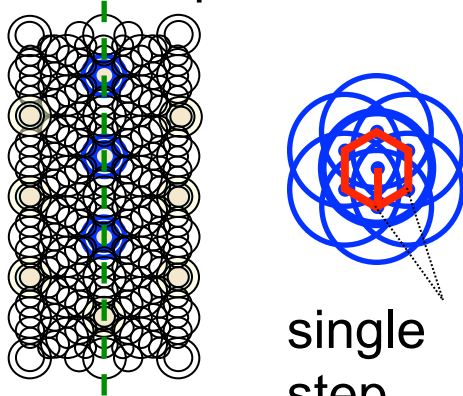
Photometer AOT

7 point jiggle (point source)

small map

scan (large) map

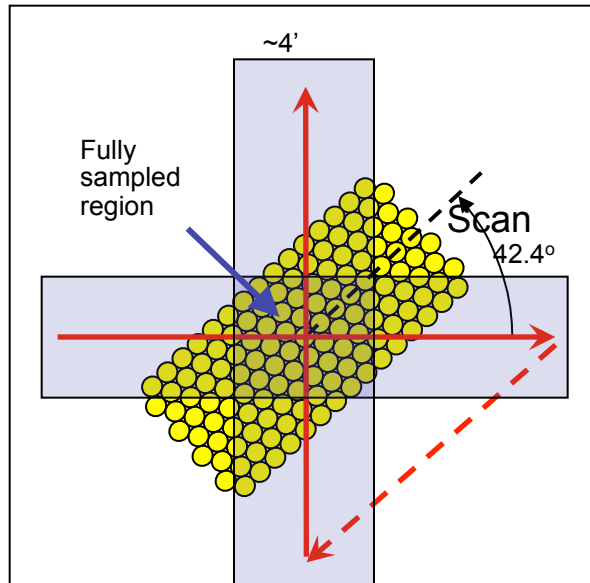
126" chop + nod



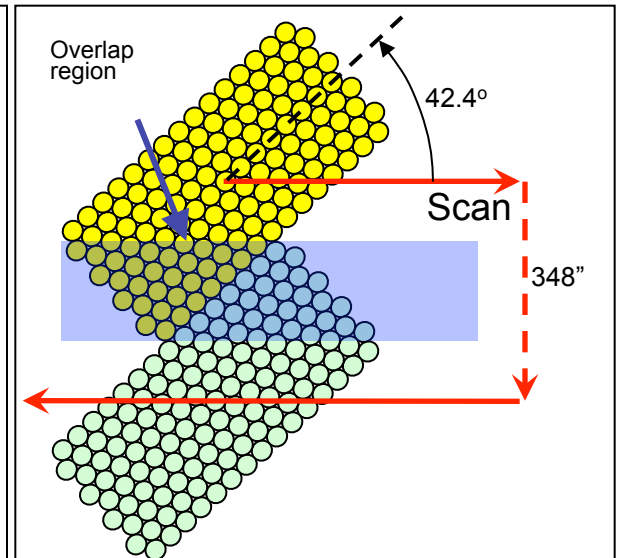
single
step
~ 6"

7-point jiggle for point source photometry, to compensate pointing error and under-sampling. Chopping and nodding at each jiggle position.

Observations exist in archive but never used for science programs.



Single cross scan at 84.8° replaces Jiggle map. Scan map at speeds of 30 and 60 "/sec. Full spatial sampling in center of scans.

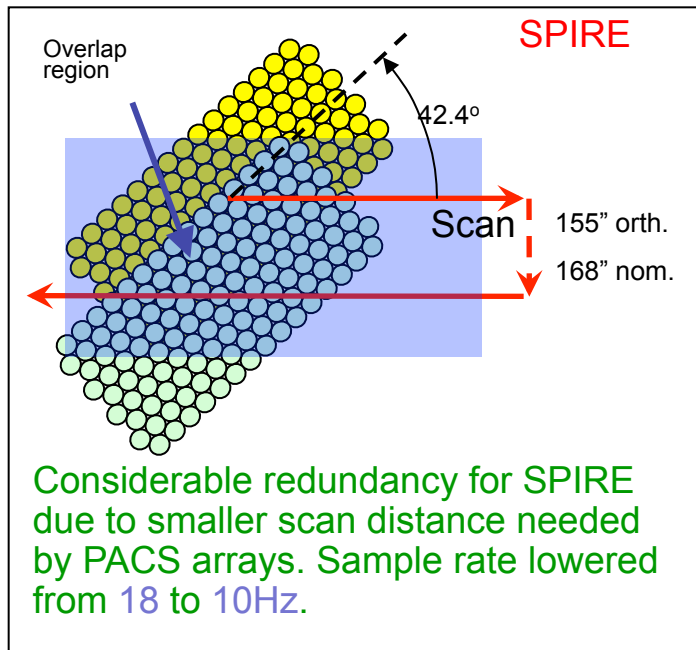


Scan map at speeds of 30 and 60 "/sec is most efficient mode for large-area surveys. Parameters are optimized for full spatial sampling and uniform distribution of integration time. Cross scan capability (84.8°)

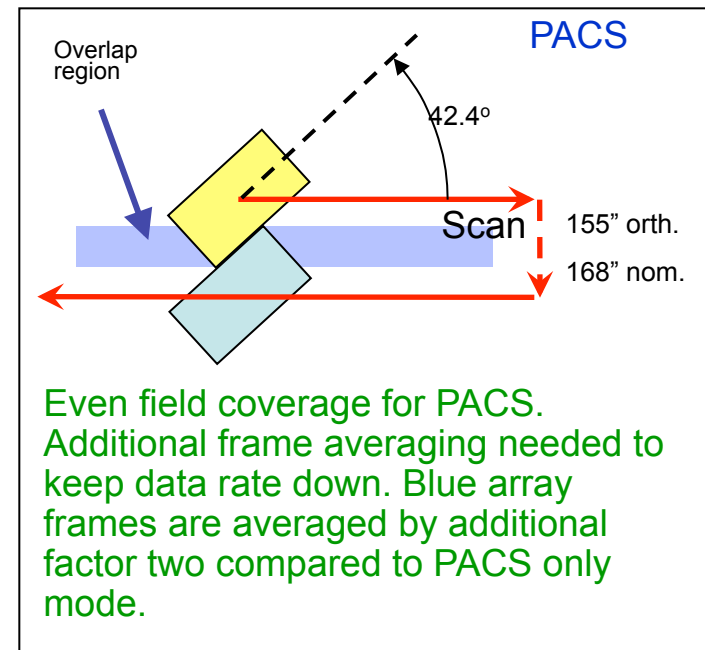
Parallel Mode SPIRE and PACS

- Scan maps at speeds of 20 and 60"/sec with PACS and SPIRE active in parallel are useful for large-area surveys.
- The distance between PACS and SPIRE apertures is 21 arcmin.
- Two almost orthogonal (84.8°) directions for cross scanning are available.

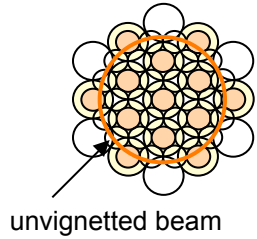
SPIRE Geometry



PACS Geometry



Spectrometer AOT



Overlapping spectrometer arrays projected on the sky

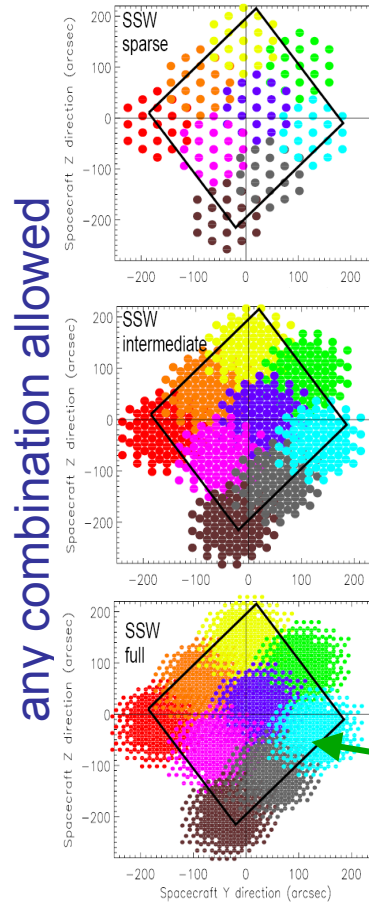
Image Sampling

- Sparse
- Intermediate
- Full

Pointing Mode

- Single Pointing
- Raster Pointing

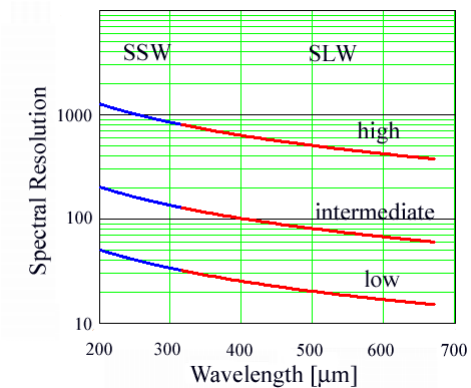
example 3 x 3 map



any combination allowed

Spectral Resolution

- High 0.04 cm^{-1}
- Medium 0.25 cm^{-1}
- Low 1.0 cm^{-1}
- High & Low $0.04/1.0 \text{ cm}^{-1}$



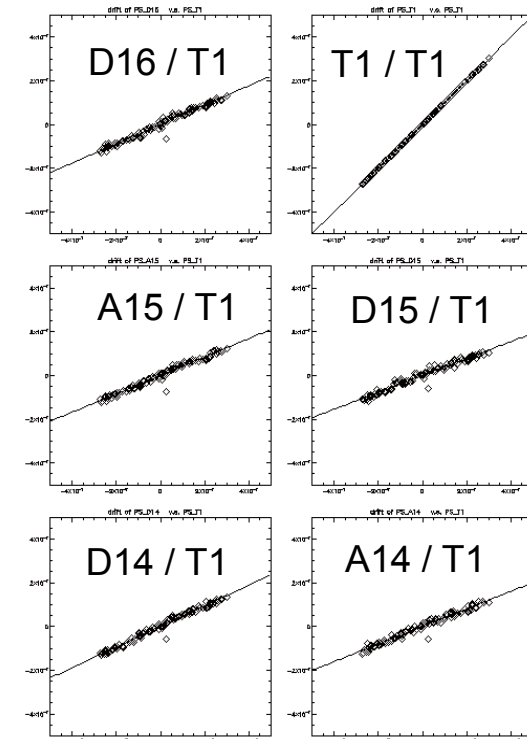
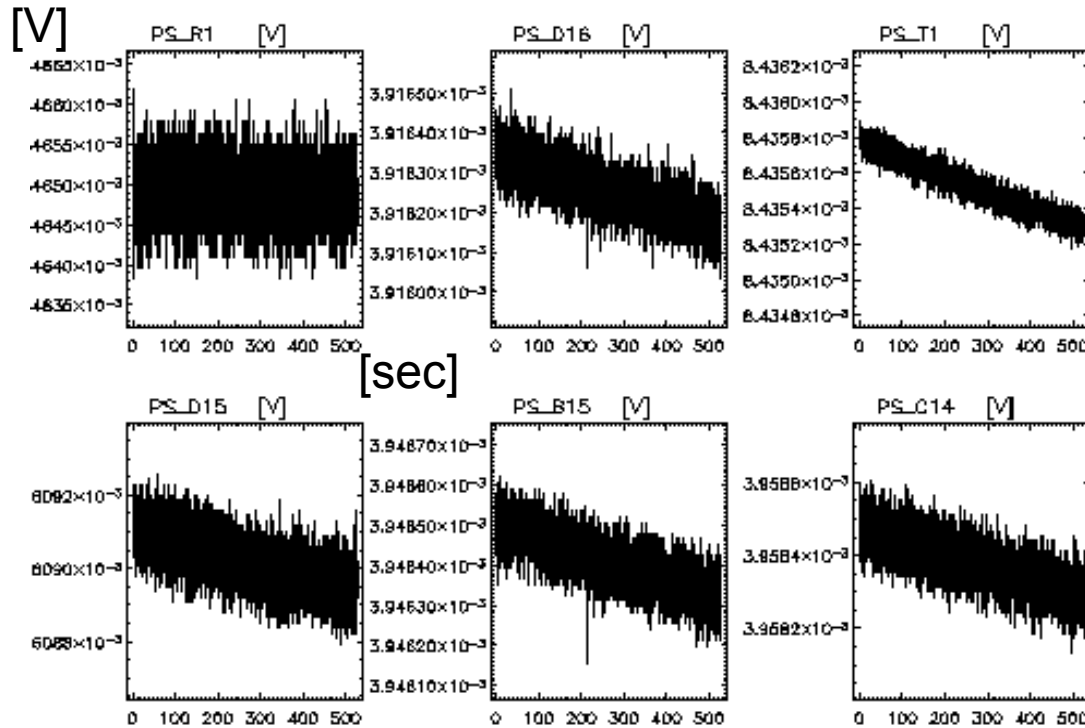
Each color shows the unvignetted beams of the same array for all sampling positions (jiggles) at one raster position.



Calibration

Detector Stability

PSW array

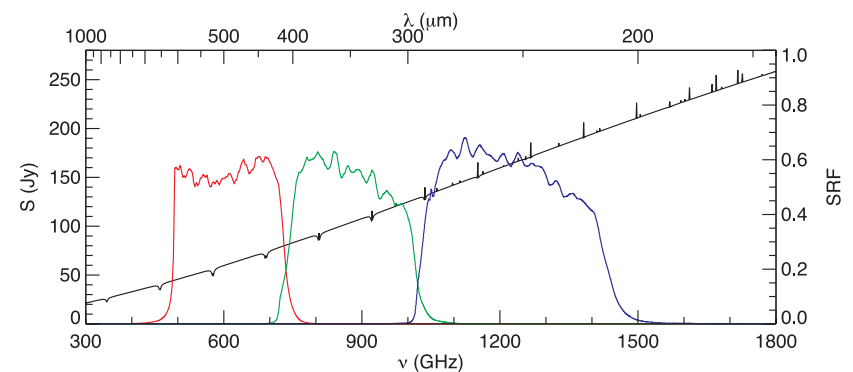
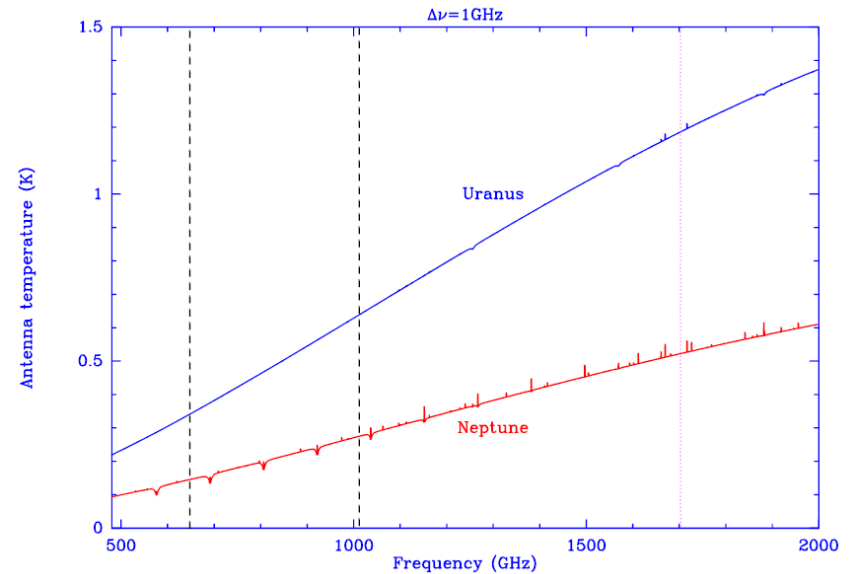


Most signal drifts come from **temperature changes**, as shown by the perfect correlation of thermistor pixel T1 and detector signals. The resistor pixel R1 does not vary with temperature.

Signal is very stable after correction with thermistor signals ($1/f$ knee $< 10\text{mHz}$).

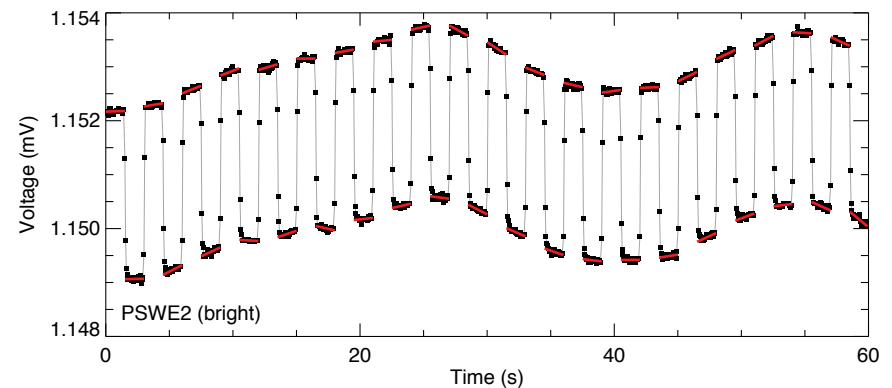
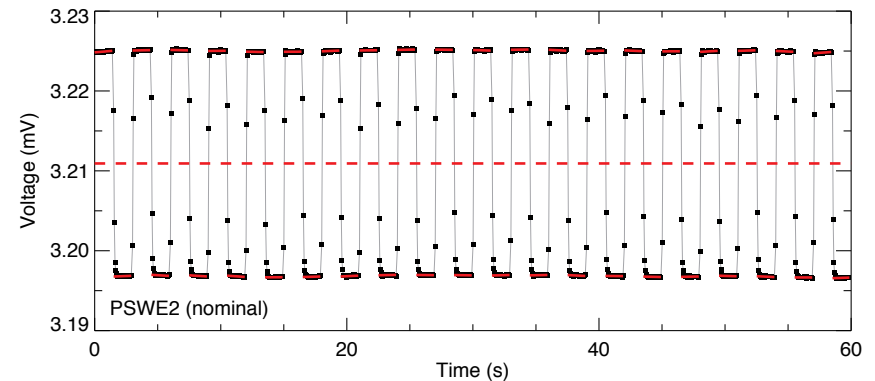
Flux Calibration

- The SPIRE flux calibration is based on the planets **Neptune**, for the photometer, and **Uranus** for the spectrometer.
- We use radiative models provided by Rafael Moreno.
- The models are estimated to be accurate to $\sim 4\%$.
- Filter spectral resolution is ~ 3 .
→ **Color correction is essential!**



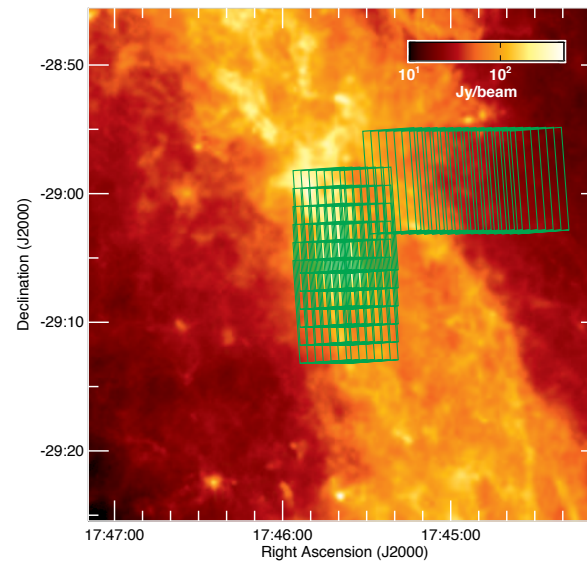
Linearity Calibration

- The **SPIRE Spiderweb bolometers** are very well understood and good model descriptions exist.
- Still, **empirical calibration** offers the highest level of accuracy.
- An **internal calibration source** (PCal) provided highly stable and reproducible infrared flashes illuminating all detectors simultaneously on top of the celestial background.
- These flashes allow to measure a **relative detector responsivity** at the current total flux level that is a sum of sky and telescope emission.
- for details see Bendo et al. 2013, MNRAS 433, 3062

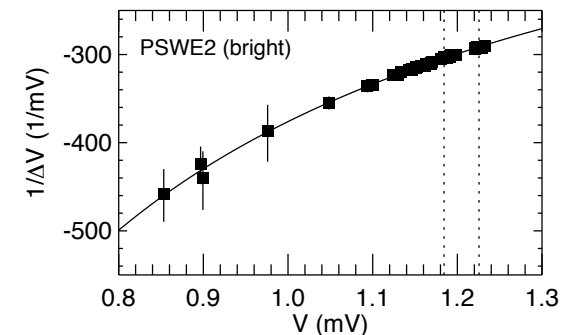
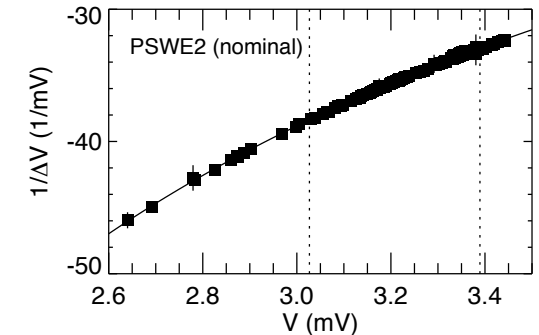


Linearity Calibration

- Each SPIRE observation contains a sequence of calibration flashes.
- Special observations in bright regions were performed to increase the statistics of data points at bright fluxes.
- Thus the flux range for each detector was serendipitously filled in and linearity curves were derived for both, **nominal**, and **bright** observing modes.



The diagrams show data from the photometer calibration, however the spectrometer linearisation is done in the same way.



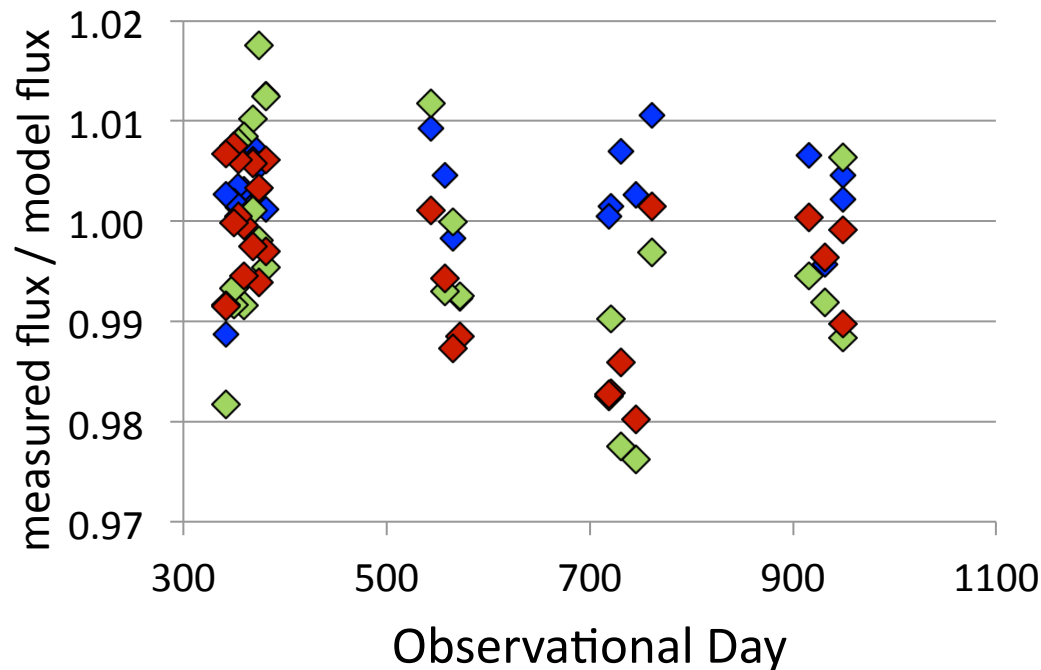
from Bendo et al. 2013,
MNRAS 433, 3062

See also Swinyard et al. 2013,
in prep.



Photometer Flux Accuracies

Photometer Reproducibility: Neptune



- Repeatability is ~2%
- Absolute accuracy of flux standard is 4%
- Conservative estimate of absolute flux calibration accuracy is 6%

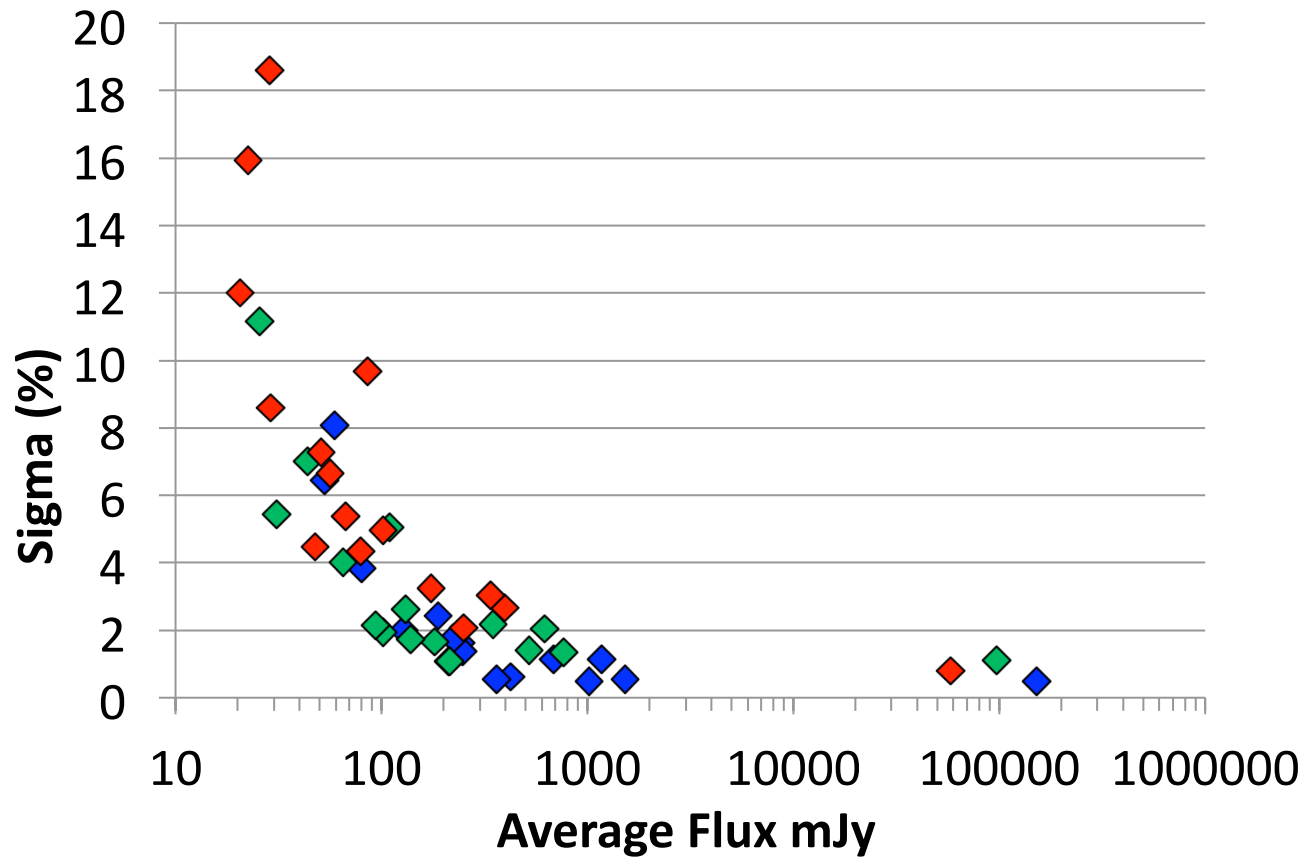
Ratio Standard Deviation:

PSW=0.005, PMW=0.011, PLW=0.008

(Lim et al. 2013 in prep.)

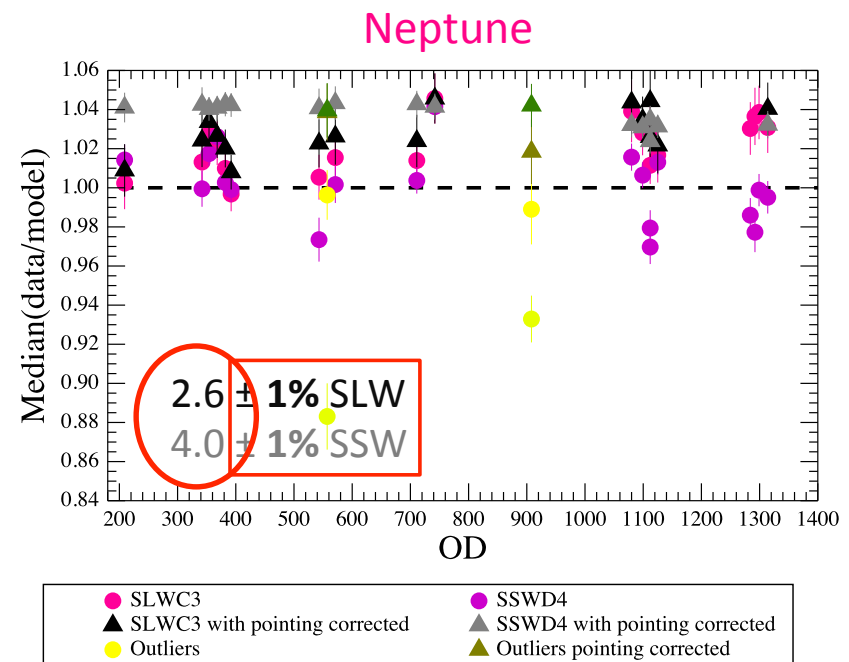
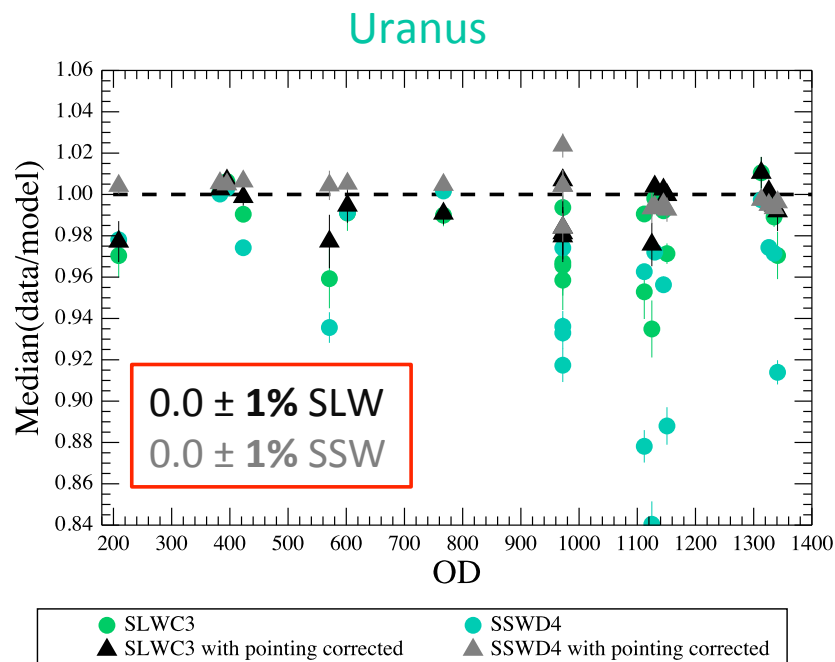


Repeatability at Stellar Fluxes





Spectrometer Flux Accuracies



Pointing offsets are more important for the spectrometer!

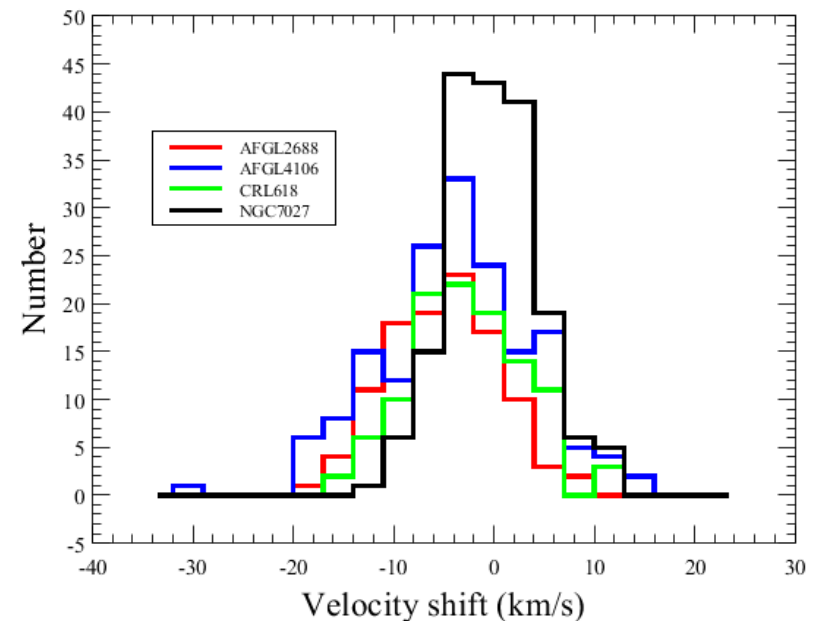


Spectrometer Flux Calibration Accuracy

- Flux Calibration Accuracy
 - 1% reproducibility of planet measurements
 - 4% uncertainty in planet models
 - 3% pointing related accuracy (SSW)
- Repeatability:
 - 1 - 6% for line flux;
 - 5 - 7 km/s for line velocity.
- Continuum flux suffers an additive term of 0.4 Jy uncertainty due to larger uncertainties in telescope emission subtraction.

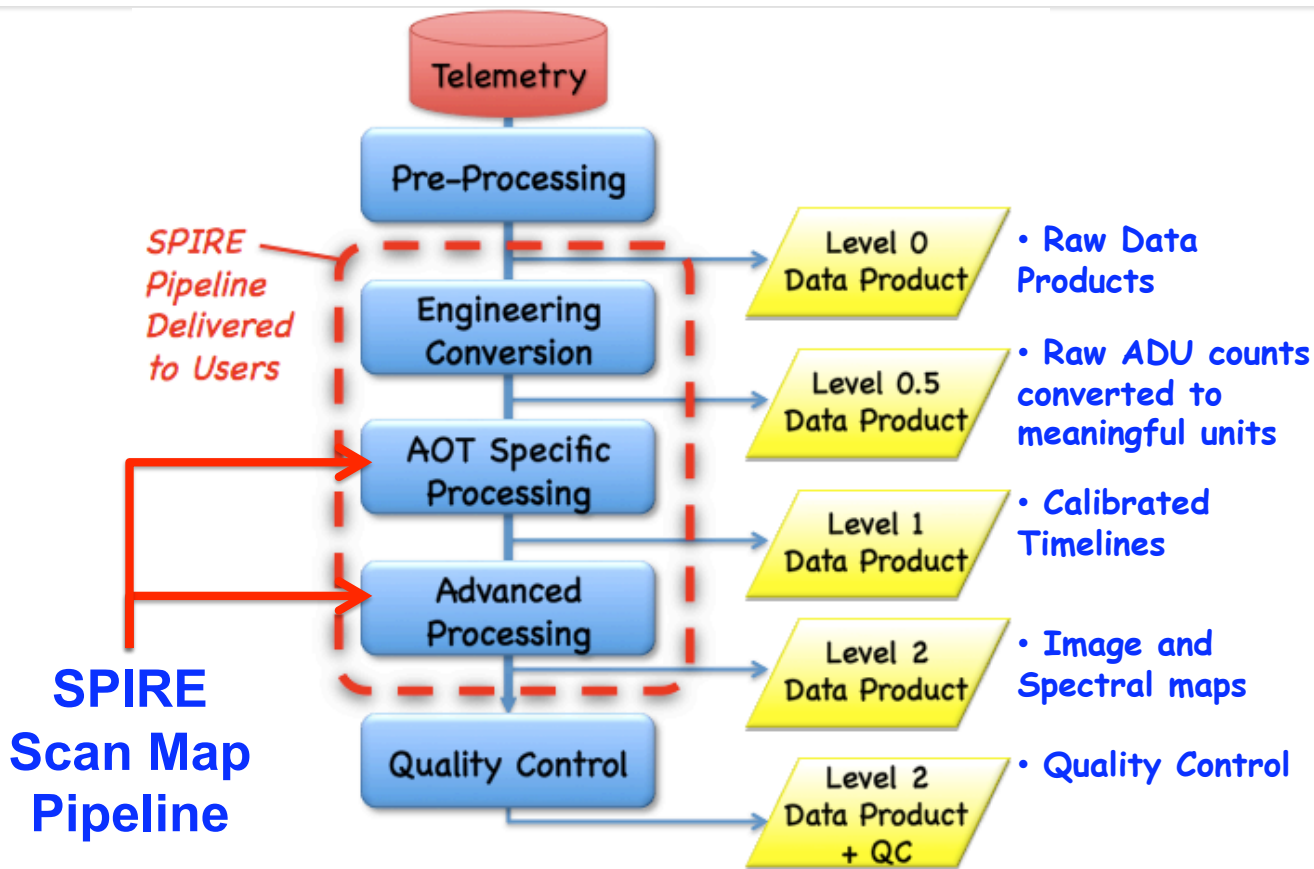
Wavelength Calibration

- Wavelength calibration was obtained from observations of the CO-ladder in the Orion Bar and checked with PNs like NGC 7027 (Swinyard et al. 2013 in prep.).
- From these observations the uncertainty is estimated to be $< 7\text{km/s}$.





Standard Processing Pipelines (PHOT)

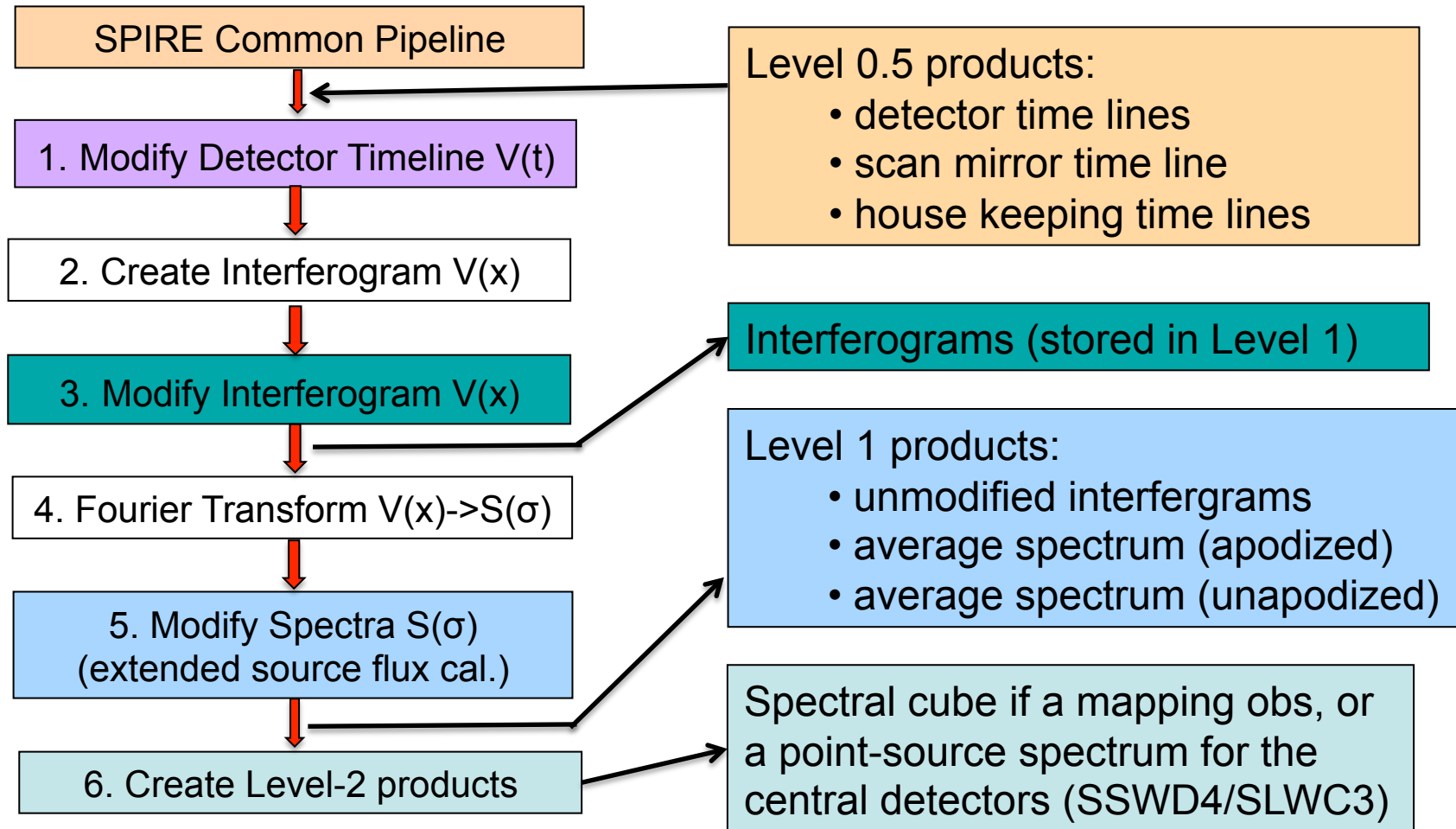


- **Level 2.5** and **Level 3.0** are products that come from combinations of more than one observation.
- **Level 2.5:** pairs of parallel mode observations
- **Level 3.0:** combinations of overlapping clusters of observations from the same proposal.

Note: This definition was different in HIPE 10. Level 2.5 was what is in Level 3.0 of HIPE 11. Level 3.0 didn't exist.



Standard Processing Pipelines (SPEC)





Demo

- Retrieve observation context from pool
- Look at Level 2 products